JOC The Journal of Organic Chemistry
Cite This: J. Org. Chem. 2019, 84, 9215−9225
Article
pubs.acs.org/joc

Formation and Reactivity of Triplet Vinylnitrenes as a Function of Ring Size

DeVonna M. Gatlin,[†] William L. Karney,[‡] Manabu Abe,[§] Bruce S. Ault,[†] and Anna D. Gudmundsdottir*[,†]

[†]Department of Chemistry, University of Cincinnati, Cincinnati, Ohio 45221, United States
[‡]Department of Chemistry, University of San Francisco, 2130 Fulton Street, San Francisco, California 94117, United States
[§]Department of Chemistry, Graduate School of Science, Hiroshima University, Hiroshima 739-8526, Japan

Supporting Information

ABSTRACT: The photoreactivity of cyclic vinyl azides **1** (3-azido-2-methyl-cyclopenten-1-one) and **2** (3-azido-2-methyl-2-cyclohexen-1-one), which have five- and six-membered rings, respectively, was characterized at cryogenic temperature with electron paramagnetic resonance (EPR), IR, and UV spectroscopy. EPR spectroscopy revealed that irradiating ($\lambda > 250$ nm) vinyl azides **1** and **2** in 2-methyltetrahydrofuran at 10 K resulted in the corresponding triplet vinylnitrenes ^{3}**1N** (D/hc = 0.611 cm^{-1} and E/hc = 0.011 cm^{-1}) and ^{3}**2N** (D/hc = 0.607 cm^{-1} and E/hc = 0.006 cm^{-1}), which are thermally stable at cryogenic temperature. Irradiation of vinyl azides **1** (310 nm light-emitting diode at 12 K) and **2** (xenon arc lamp through a 310−350 nm filter at 8 K) in argon matrices showed that in competition with intersystem crossing to form vinylnitrenes ^{3}**1N** and ^{3}**2N**, vinyl azide **1** formed a small amount of ketenimine **3**, whereas vinyl azide **2** formed significant amounts of azirine **7** and ketenimine **6**. Thus, vinyl azide **1** undergoes intersystem crossing more efficiently than vinyl azide **2**. Similarly, vinylnitrene ^{3}**1N** is much more photoreactive than vinylnitrene ^{3}**2N**. Quantum chemical calculations were used to support the mechanisms for forming vinylnitrenes ^{3}**1N** and ^{3}**2N** and their reactivity.

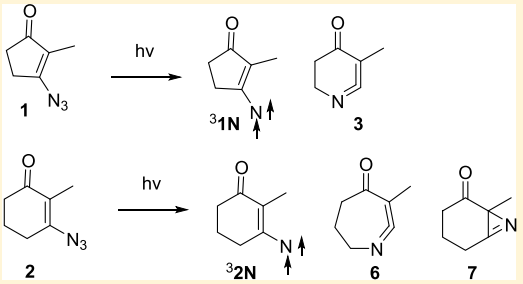

INTRODUCTION

Vinyl azides and 2*H*-azirines are versatile functional groups that can be used to form new C−N bonds in synthetic applications.[1] The dipolar character of vinyl azides makes them suitable for cycloaddition to alkynes and olefins, which has been used successfully in countless syntheses.[2−8] Similarly, 2*H*-azirine derivatives can undergo cycloaddition to alkenes, but more importantly, they can react as both nucleophiles and electrophiles. Because azirines are highly reactive owing to their intrinsic ring strain, they are valuable building blocks in synthesis.[9,10] The quest for sustainable chemistry has attracted attention to the use of sunlight, a natural resource, or energy-efficient light-emitting diodes (LEDs) for synthetic applications.[11,12] For example, photocatalytic sensitization of aryl and vinyl azides has been successfully used for selective C−N bond formation.[13,14] However, the synthetic utility of the photochemistry of vinyl azide and 2*H*-azirine derivatives is limited by their complex photoreactivity, which depends on multiple factors, such as molecular structure, irradiation wavelength, and whether excitation occurs directly or with sensitizers.[15−18] For example, direct irradiation of vinyl azide chromophores can yield azirines in a concerted manner on the singlet excited surface, whereas triplet sensitization yields triplet vinylnitrene intermediates (Scheme 1).[19,20] In comparison, direct irradiation of 2*H*-azirines results in the formation of the corresponding ylide, whereas triplet sensitization leads to C−N bond cleavage to form vinylnitrenes.[21−23] Thus, to use the photoreactivity of vinyl azide or 2*H*-azirine derivatives in synthetic applications for C−N bond formation, it is important to be able to control their photochemistry, which can only be achieved by understanding their reactivity. Evaluating whether triplet vinylnitrenes are involved in a reaction is challenging because they are generally short-lived intermediates that decay efficiently by intersystem crossing to form products or to reform the starting material, and, thus, it is necessary to rely on

Scheme 1

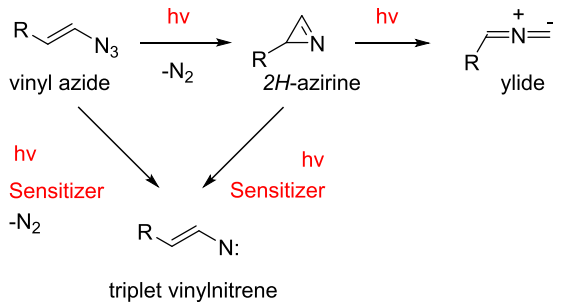

Received: May 2, 2019
Published: July 2, 2019

DOI: 10.1021/acs.joc.9b01191
J. Org. Chem. 2019, 84, 9215−9225

spectroscopy for their identification.[24] A further complication in characterizing triplet vinylnitrenes is that they are not stable at low temperatures, unless they are a part of a cyclic structure.[25,26]

In this article, we compare the reactivity of two cyclic vinyl azide derivatives, 3-azido-2-methyl-2-cyclopenten-1-one (**1**, Scheme 2) and 3-azido-2-methyl-2-cyclohexen-1-one (**2**, Scheme 2), in cryogenic matrices. We specifically studied these vinyl azides, which have built-in triplet sensitizer or ketone chromophore, to form triplet vinylnitrenes, which are not conjugated to aromatic rings. We demonstrate that irradiation of both vinyl azides **1** and **2** with UV light results in the formation of the corresponding triplet vinylnitrenes, ^{3}**1N** and ^{3}**2N**. The ring size of vinylnitrenes ^{3}**1N** and ^{3}**2N** (Scheme 2) affects their formation and reactivity but not their biradical character.

Scheme 2

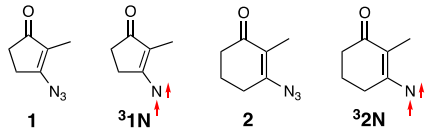

RESULTS

Electron Paramagnetic Resonance (EPR) Spectroscopy. EPR spectroscopy verified that exposure of vinyl azides **1** and **2** to UV light in 2-methyltetrahydrofuran (mTHF) at 10 K yields the corresponding vinylnitrenes, ^{3}**1N** and ^{3}**2N**. The spectrum of ^{3}**1N** shows X_2 and Y_2 signals at 5534 and 5988 Gauss, respectively, at a resonance frequency of 9.4 GHz, whereas the spectrum of ^{3}**2N** has X_2 and Y_2 signals at 5623 and 5873 Gauss, respectively (Figure 1). The zero-field splitting (zfs) parameters for vinylnitrenes ^{3}**1N** and ^{3}**2N** were calculated using the X_2 and Y_2 signals of each spectrum according to the Wasserman equations.[27] The calculated zfs parameters for vinylnitrene ^{3}**1N** are D/hc = 0.611 cm^{-1} and E/hc = 0.011 cm^{-1}, whereas those for ^{3}**2N** are D/hc = 0.607 cm^{-1} and E/hc = 0.006 cm^{-1}. The X_2 and Y_2 signals observed for vinylnitrenes ^{3}**1N** and ^{3}**2N** are characteristic of triplet vinylnitrenes, and the D/hc values demonstrate that vinylnitrenes ^{3}**1N** and ^{3}**2N** have a significant 1,3-biradical character.[25,26] It is noteworthy that vinylnitrene ^{3}**1N** has a larger deviation from the cylindrical symmetry of the spins than that of ^{3}**2N**, and, thus, the EPR spectra of ^{3}**1N** and ^{3}**2N** have different shapes.

Wentrup and co-workers have shown that most reported triplet nitrenes exhibit a linear correlation between their measured D values and the UB3LYP-calculated natural spin densities on the nitrogen atoms.[28−30] The zfs values for vinylnitrenes ^{3}**1N** and ^{3}**2N** also fit this trend (vide infra).

The EPR signal intensities grew as a function of irradiation time, and no new signals were observed upon further irradiation. The EPR spectra of vinylnitrene ^{3}**1N** broadened as the matrix was warmed to 80 K. However, upon recooling, the intensity was recovered, thus, verifying that vinylnitrene ^{3}**1N** is stable up to at least 80 K (Figure 1b). Similarly, vinylnitrene ^{3}**2N** is also stable up to 80 K (Figure 1d), as the intensity of the spectra was recovered upon recooling. However, at temperatures above 40 K, the signals from the cavity of the EPR spectrometer become more intense than the signals due to vinylnitrene ^{3}**2N**.

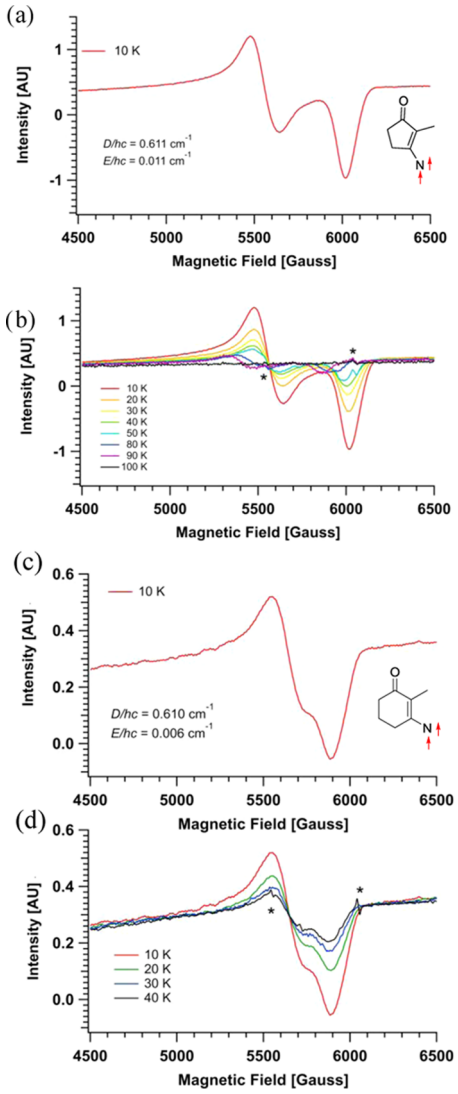

Figure 1. (a) EPR spectrum obtained by irradiating (λ > 250 nm) vinyl azide **1** in mTHF at 10 K. (b) EPR signals of ^{3}**1N** as a function of temperature. (c) EPR spectrum obtained by irradiating (λ > 250 nm) vinyl azide **2** in mTHF at 10 K. (d) EPR signals of ^{3}**2N** as a function of temperature. Signals due to the cavity of the EPR spectrometer are labeled with *.

UV Absorption in Glassy mTHF Matrices. To further characterize vinylnitrenes ^{3}**1N** and ^{3}**2N**, their UV−vis spectra were obtained in glassy mTHF matrices at 77 K. Figure 2 displays the difference absorption spectra of vinyl azides **1** and **2** as a function of irradiation time. Vinyl azide **1** was irradiated with an LED (~310 nm), and vinyl azide **2** was irradiated through a Pyrex filter (>300 nm). As vinyl azides **1** and **2** were exposed to light, new broad absorption bands were formed with λ_{max} at ~235 and 398 nm, and at ~236 and ~368 nm, respectively. These bands, which increased throughout irradiation (Figure 2), are assigned to vinylnitrenes ^{3}**1N** and ^{3}**2N** by comparison to their time-dependent density functional theory (TDDFT)-calculated spectra. At the TD-B3LYP-(IPCM,THF)/6-31+G* level, the major calculated electronic transitions for vinylnitrene ^{3}**1N** are located at 410 (f = 0.002), 358 (f = 0.03), 281 (f = 0.02), 277 (f = 0.0039), and 238 (f = 0.1471) nm, whereas the major bands for ^{3}**2N** are at located 402 (f = 0.0012), 344 (f = 0.0141), 282 (f = 0.0007), 276 (f =

DOI: 10.1021/acs.joc.9b01191
J. Org. Chem. 2019, 84, 9215−9225

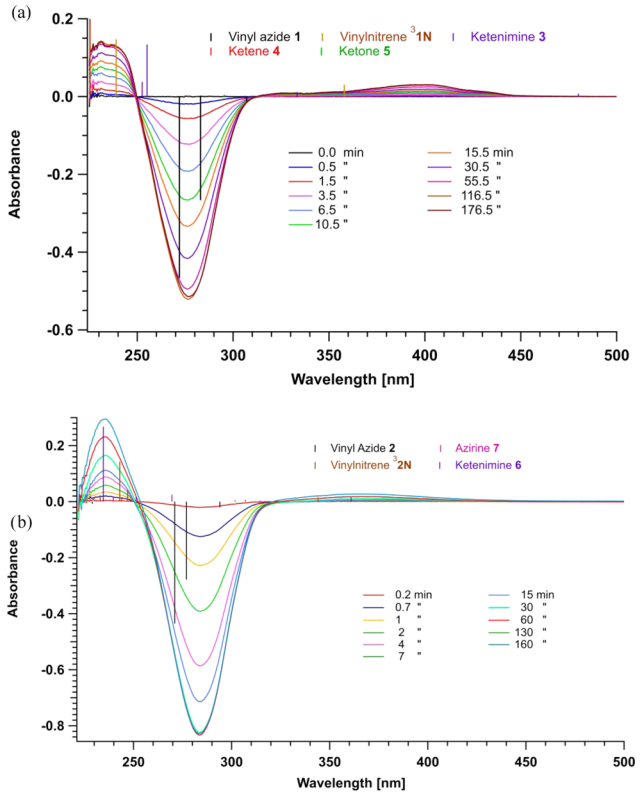

Figure 2. UV−vis difference spectra obtained by irradiating (λ > 250 nm) vinyl azides (a) **1** and (b) **2** in mTHF matrices at 77 K. TDDFT-calculated electronic transitions are shown as bars for the S_0 of **1** and **2** and for vinylnitrenes ^{3}**1N** and ^{3}**2N**, ketenimines **3** and **6**, azirine **7**, ketene **4**, and ketone **5**. The 4 and 7 min traces have some overlaps.

0.0011), 247 (f = 0.041), 244 (f = 0.0116), and 243 (f = 0.1427) nm. Additional support for these assignments was provided by the electronic transitions computed by multistate CASPT2 calculations (Table 1). The CASPT2 prediction of relatively strong transitions around 360 nm for the triplet nitrenes agrees reasonably well with the density functional theory (DFT) results, although the agreement is not as good in the remainder of the spectrum. In particular, CASPT2 does not yield a strong excitation in the region of 240 nm. One possible reason for this poor correspondence is that the accurate prediction of electronic transitions with CASPT2 requires a very large active space that includes many sigma molecular orbitals (MOs), but such calculations exceeded our computational resources. Another possible explanation is that the isodensity polarizable continuum model (IPCM) solvation model used for the TDDFT calculations is not available for use with the CASPT2 calculations.

Table 1. CASPT2(12,11)/cc-pVDZ//B3LYP/6-31+G* Computed Electronic Transitions and Oscillator Strengths for Vinylnitrenes ^{3}1N and ^{3}2N[a]

species	λ (nm)	f
^{3}**1N**	656	0.000025
	359	0.012
	277	0.0013
	261	0.00051
	253	0.000055
	229	0.000057
^{3}**2N**	656	0.000093
	363	0.0045
	304	0.0010
	285	0.00016
	273	0.00054
	258	0.000036
	235	0.000071

[a]Using state-averaged CASSCF and multistate CASPT2 calculations.

The negative bands in Figure 2 are due to the depletion of vinyl azides **1** and **2**, as supported by the agreement between the observed and calculated TDDFT absorption spectra. Although the absorption observed at longer wavelengths in the spectra in Figure 2 can be assigned to triplet vinylnitrenes ^{3}**1N** and ^{3}**2N**, it is not possible to exclude the possibility that other photoproducts are also formed concurrently with the vinylnitrenes or by secondary photolysis.

Matrix Isolation. As EPR and UV-vis absorption spectroscopy show that vinylnitrenes ^{3}**1N** and ^{3}**2N** have remarkably similar properties, we investigated whether their ring sizes affected their formation and reactivity by using matrix isolation and IR spectroscopy to identify any products formed concurrently with the vinylnitrenes and their secondary photoreactivity.

Vinyl azide **1** was irradiated with a 310 nm LED for a total of ∼115.5 min in an argon matrix at 12 K, and IR spectra were recorded at various time intervals. The bands of vinyl azide **1** at 2109, 1720, 1653, 1385, 1335, 1269, 1139, 827, and 627 cm^{-1} were depleted upon irradiation (Figure 3a). Concurrently, new bands with contrasting time profiles were formed, suggesting primary and secondary photochemical reactions. The bands that formed at 1659 and 1369 cm^{-1} increased for the first 55 min of irradiation and then decreased somewhat upon further irradiation. These bands were assigned to vinylnitrene ^{3}**1N** based on comparison to its calculated IR spectrum. The calculated frequencies of the C═O and the coupled C═C and C−N stretching bands were located at 1630 and 1316 cm^{-1} after scaling by 0.9613,[31] which is in good agreement with the experimental IR bands (Figure 3b). In addition, the less intense bands at 1026, 982, and 648 cm^{-1} were also assigned to vinylnitrene ^{3}**1N**, as they exhibited the same time profile as the bands at 1659 and 1369 cm^{-1}, and they corresponded to the calculated and scaled frequencies at 1046, 959, and 628 cm^{-1}.

Concurrently with the formation of vinylnitrene ^{3}**1N**, bands appeared at 1871, 1867, 1863, and 1662 cm^{-1}. The intensities of these bands increased with further irradiation, and there was no indication of secondary photoreactions. We assigned these bands to ketenimine **3** based on the comparison to its calculated spectrum, in which the most significant bands were calculated and scaled to be at 1899 and 1658 cm^{-1}, corresponding well with the observed bands. The C═C═N bands at 1871, 1867, and 1863 cm^{-1} in the spectrum of **3** must be due to different conformers of ketenimine **3** or different sites in the argon matrices.

After irradiation of vinyl azide **1** for ∼10 min, additional new bands were formed at 2230, 2145, 1818, 1813, 1602, 1464, 1436, 1193, 993, 957, and 943 cm^{-1}, which grew with further irradiation. Because these bands continued to grow after the intensity of the vinylnitrene ^{3}**1N** bands decreased, they are assigned to secondary photoproducts from vinylnitrene ^{3}**1N**. These bands were assigned to ketene **4** and ketone **5** by comparison to their calculated spectra. The bands at 2145, 1602, 1193, 993, and 943 cm^{-1} assigned to ketene **4** fit well with the calculated and scaled bands at 2106, 1564, 1217,

DOI: 10.1021/acs.joc.9b01191
J. Org. Chem. 2019, 84, 9215−9225

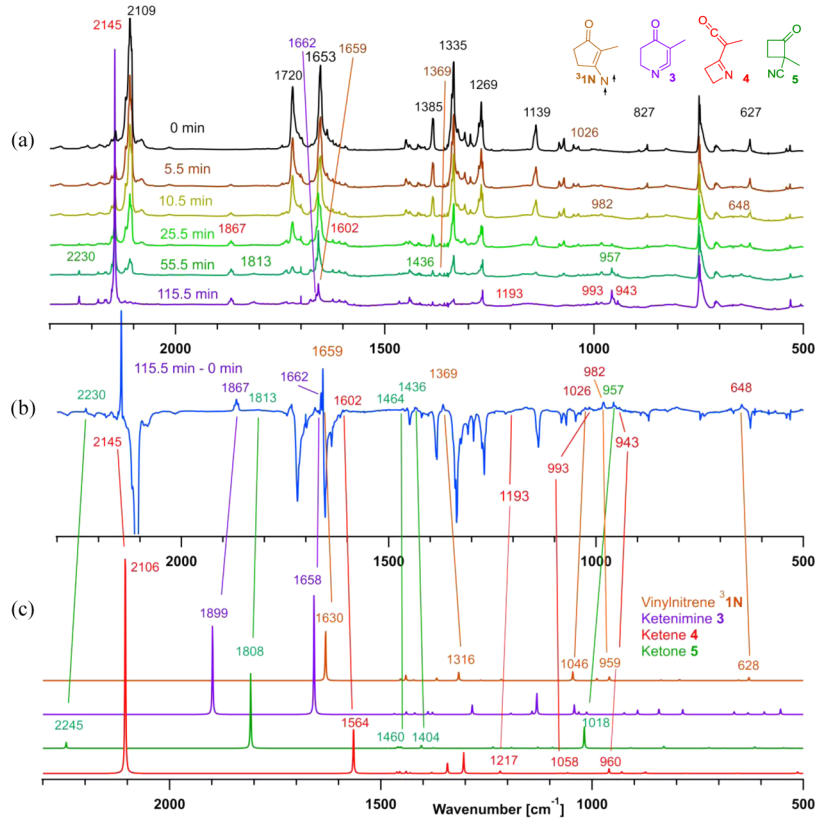

Figure 3. (a) IR spectra obtained before and after various periods of irradiation of vinyl azide **1** with a 310 nm LED in an argon matrix at 12 K. (b) Difference spectrum obtained by subtracting the IR spectrum of vinyl azide **1** from the one obtained after 115.5 min of irradiation. (c) B3LYP/6-31+G(d)-calculated IR spectra of vinylnitrene ^{3}**1N**, ketenimine **3**, ketene **4**, and ketone **5**. Difference spectra obtained at various irradiation times, and various expansions of the spectra and difference spectra can be found in the Supporting Information (SI) (Figures S1−S6). The formation of azirine **8** from photolysis of vinyl azide **1** was ruled out based on the comparison to its calculated and scaled IR spectrum (see Figure S1 in the SI).

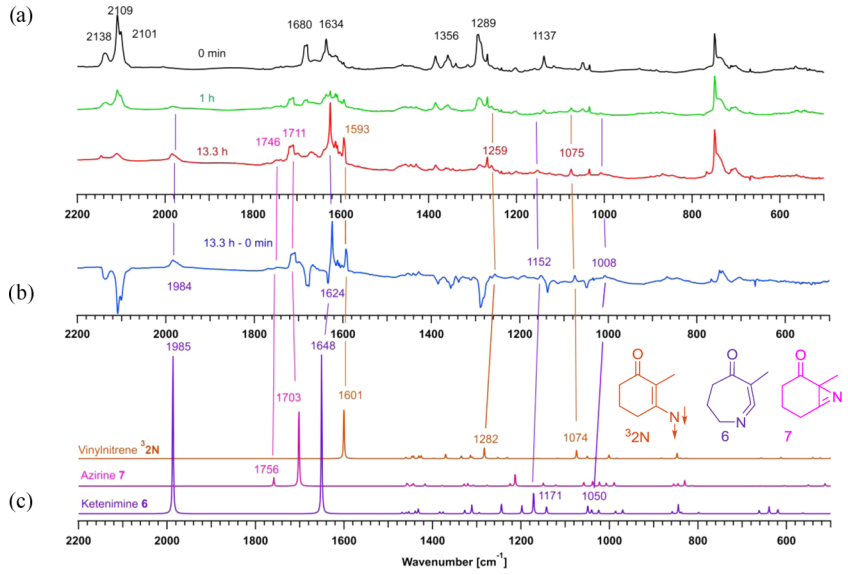

Figure 4. (a) IR spectra obtained before and after various periods of irradiation of vinyl azide **2** with a xenon arc lamp through a 310−350 nm glass filter in an argon matrix at 8 K. (b) Difference spectrum obtained by subtracting the IR spectrum of vinyl azide **2** from the one obtained after 13.3 h of irradiation. (c) B3LYP/6-31+G(d)-calculated IR spectra of vinylnitrene ^{3}**2N**, ketenimine **6**, and azirine **7**. Difference spectra obtained at various irradiation times can be found in the SI (Figures S6 and S7).

1058, and 960 cm^{-1}, whereas the bands at 2230, 1818, 1813, 1464, 1436, and 957 cm^{-1} were assigned tentatively to ketone **5** based on its calculated and scaled bands at 2245, 1808, 1460, 1404, and 1018 cm^{-1}. The C═O bands at 1818 and 1813 cm^{-1} in the spectrum of ketone **5** must be due to different conformers of **5** or different sites in the argon matrices. In addition, the IR spectrum of neat ketone **5** has been reported to have a CN stretch at 2235 cm^{-1} and a C═O stretch at 1800

DOI: 10.1021/acs.joc.9b01191
J. Org. Chem. 2019, 84, 9215−9225

Scheme 3. Proposed Mechanism for the Formation of Vinylnitrene ^{3}1N and Photoproducts 3−5 from the Photolysis of Vinyl Azide 1

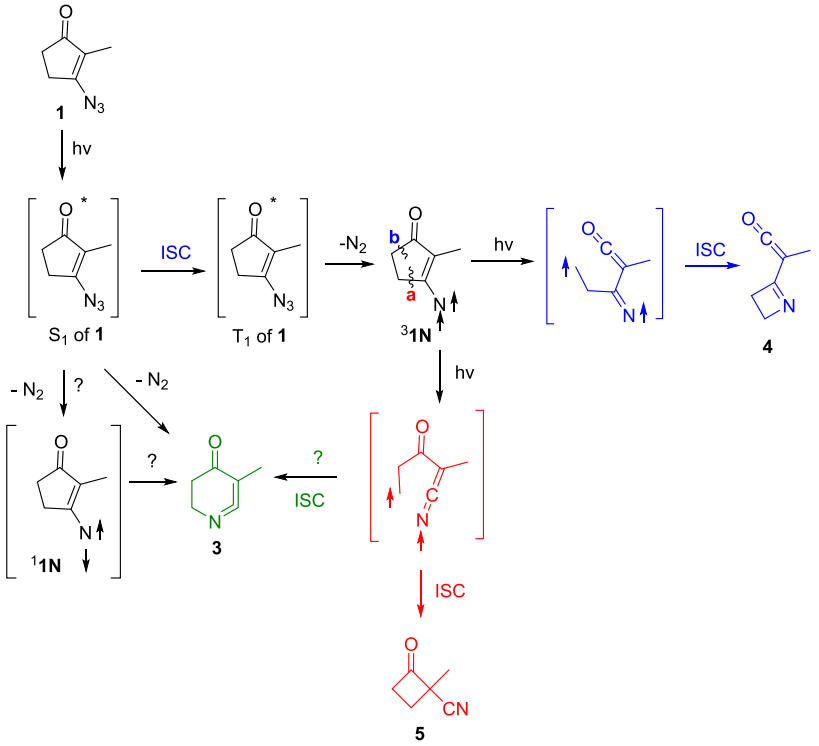

cm^{-1},[32] which are shifted by 5 and 13 to 18 cm^{-1}, respectively, relative to the bands observed in matrices. However, these shifts are likely due to the polar medium of neat ketone **5**, whereas the matrix spectrum shows better correspondence with the calculated gas-phase IR spectrum.

Vinyl azide **2** was irradiated through a 310−350 nm glass filter for ∼13 h (Figure 4) in argon matrices at 8 K. IR spectra were obtained at various time intervals (5 min, 10 min, 1 h, 2 h, 2.5 h, 4.0 h, 4.8 h, and 13.3 h) to follow the progress of the photolysis (the spectra are displayed in the SI). The IR bands corresponding to vinyl azide **2** at 2138, 2109, 2101, 1680, 1634, 1356, 1289, and 1137 cm^{-1} were almost fully depleted upon exposure to light for 13.3 h. As these bands were depleted, new bands were concurrently formed, with the most significant ones appearing at 1984, 1746, 1711, 1624, 1593, 1259, 1152, 1075, and 1008 cm^{-1}. These bands were assigned to vinylnitrene ^{3}**2N**, ketenimine **6**, and azirine **7** based on the comparison to their calculated spectra. The band at 1593 cm^{-1} was assigned to the C═O band of vinylnitrene ^{3}**2N**, which is calculated (after scaling) to be at 1601 cm^{-1}. The bands observed at 1259 and 1075 cm^{-1} were also assigned to vinylnitrene ^{3}**2N**, matching well with the calculated and scaled bands at 1282 and 1074 cm^{-1}.

Furthermore, a strong band is calculated for ketenimine **6** at 1985 cm^{-1} (scaled), which matches very well with the strong, broad adsorption observed at 1984 cm^{-1}. This is a region characteristic of the antisymmetric stretching of ketenimines.[33] The band at 1624 cm^{-1} was assigned to the C═O stretch of **6**, which was calculated and scaled to be at 1648 cm^{-1}. In addition, the bands at 1152 and 1008 cm^{-1} were assigned to coupled CH_3 stretching bands in ketenimine **6**, which were calculated and scaled to be at 1171 and 1050 cm^{-1}.

Finally, the bands at 1746 and 1711 cm^{-1} were assigned to azirine **7**. The C═N and C═O bands of azirine **7** were calculated and scaled to be at 1756 and 1703 cm^{-1}, which fits well with the observed bands.

Irradiation of vinyl azide **1** in argon matrices resulted in the formation of ketenimine **3** and vinylnitrene ^{3}**1N** as the primary photoproducts. Further irradiation caused vinylnitrene ^{3}**1N** to cleave to form secondary products **4** and **5**. Because ketenimine **3** and vinylnitrene ^{3}**1N** were formed concurrently, and EPR spectroscopy showed that vinylnitrene ^{3}**1N** is thermally stable, ketenimine **3** is expected to originate from the singlet excited state (S_1) of vinyl azide **1**, which also intersystem crosses to form vinylnitrene ^{3}**1N**. It should also be mentioned, it is possible that S_1 of **1** forms singlet vinylnitrene ^{1}**1N** that yields ketenimine **3**. Furthermore, it is possible that a fraction of ketenimine **3** is produced by a secondary photoreaction of vinylnitrene ^{3}**1N** (Scheme 3). The proposed mechanism for the photoreactivity of vinyl azide **1** in matrices is depicted in Scheme 3.

In comparison, irradiation of vinyl azide **2** in matrices resulted in ketenimine **6** and azirine **7**, concurrent with the formation of vinylnitrene ^{3}**2N**. These results contrast with those for vinyl azide **1**, which did not produce an observable azirine upon irradiation. Thus, we theorize that both ketenimine **6** and azirine **7** are formed from the S_1 of **2**, which also intersystem crosses to vinylnitrene ^{3}**2N**. As before, we cannot rule out that S_1 of **2** forms a singlet vinylnitrene ^{1}**2N** that yields ketenimine **6** and azirine **7**. Scheme 4 displays the proposed pathways for the product formation from vinyl azide **2** upon irradiation in argon matrices.

As mentioned earlier, the absorption spectra obtained by irradiation of vinyl azide **1** in glassy mTHF matrices yielded absorption bands that were assigned to vinylnitrene ^{3}**1N** based on the comparison to its calculated TDDFT spectra. Furthermore, as the TD-B3LYP(IPCM,THF)-calculated spectrum of ketenimine **3** had electronic transitions at 480 (f =

DOI: 10.1021/acs.joc.9b01191
J. Org. Chem. 2019, 84, 9215−9225

Scheme 4. Proposed Mechanism for the Formation of Vinylnitrene ^{3}2N and Photoproducts 6 and 7 from the Photolysis of Vinyl Azide 2

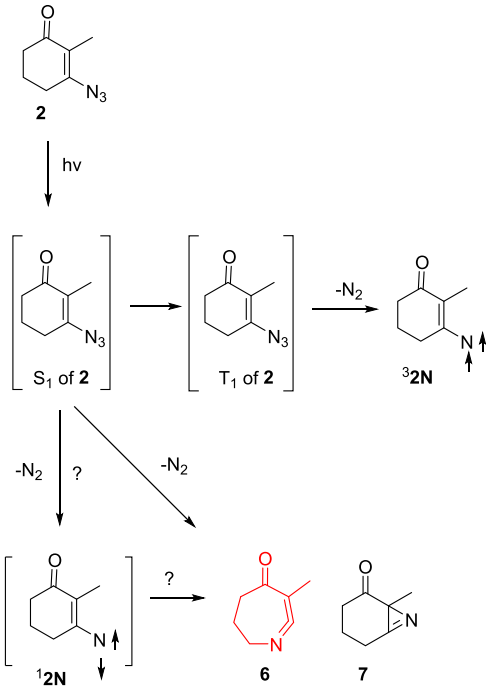

0.0075), 333 (f = 0.017), 255 (f = 0.0134), and 256 (f = 0.03878) nm, it must be formed with vinylnitrene ^{3}**1N**. However, it was difficult to identify the secondary photoproducts ketene **4** and ketone **5** from the absorption spectra (Figure 2a), because the irradiation was stopped before the new absorption bands were depleted. In comparison, irradiation of azide **2** yielded absorption spectra that could be attributed to vinylnitrene ^{3}**2N**, as stated earlier, and also ketenimine **7** and azirine **6**, which have major calculated absorbance bands at 361 (f = 0.015), 302 (f = 0.0045), 251 (f = 0.0184), 234 (f = 0.2674), 314 (f = 0.0046), 270 (f = 0.0249), 240 (f = 0.0188), and 213 (f = 0.256) nm, respectively. Thus, the results obtained by irradiating vinyl azides **1** and **2** in argon matrices and in glassy mTHF matrices are in agreement.

Quantum Chemical Calculations. DFT calculations (B3LYP/6-31+G(d)) were performed to better understand why vinylnitrenes ^{3}**1N** and ^{3}**2N** react differently in argon matrices. Optimization of the structure of vinyl azide **1** yielded two minimal energy conformers, **1A** and **1B**, differing mainly in the orientation of the azide group (Figure 5). The energies of the S_1 of **1** and its triplet excited state (T_1) were located with TDDFT calculations to be at 84 and 63 kcal/mol above its ground state (S_0) (Figure 6).

Figure 6 shows the DFT-computed relative energies of the different electronic states of each azide, along with the corresponding nitrenes and related isomers. The optimized structure of vinylnitrene ^{3}**1N** and a N_2 molecule was located 3 kcal/mol below the S_0 of **1**. Because vinylnitrene ^{3}**1N** is more stable than ketenimine **3** and azirine **8** (Figure 7), we theorize that it does not intersystem cross to form **3** or **8** at cryogenic temperature. This finding further supports the idea that azirine **8** and ketenimine **3** arise from the excited singlet reactivity of vinyl azide **1**. We were not able to optimize the T_1 of **1** or the transition state for forming vinylnitrene ^{3}**1N** from the T_1 of **1**, indicating that the energy barrier for forming vinylnitrene ^{3}**1N** must be very small.

Similarly, two minimum energy conformers, **2A** and **2B**, were optimized for vinyl azide **2**, and TDDFT calculations located its S_1 and T_1 to be at 82 and 63 kcal/mol above its S_0, respectively (Figure 6). Similar to vinyl azide **1**, we could not optimize the T_1 of **2** or the transition state connecting the T_1 of **2** to vinylnitrene ^{3}**2N**. Interestingly, vinylnitrene ^{3}**2N** is less stable than ketenimine **6** and azirine **7** (Figure 7); however, as

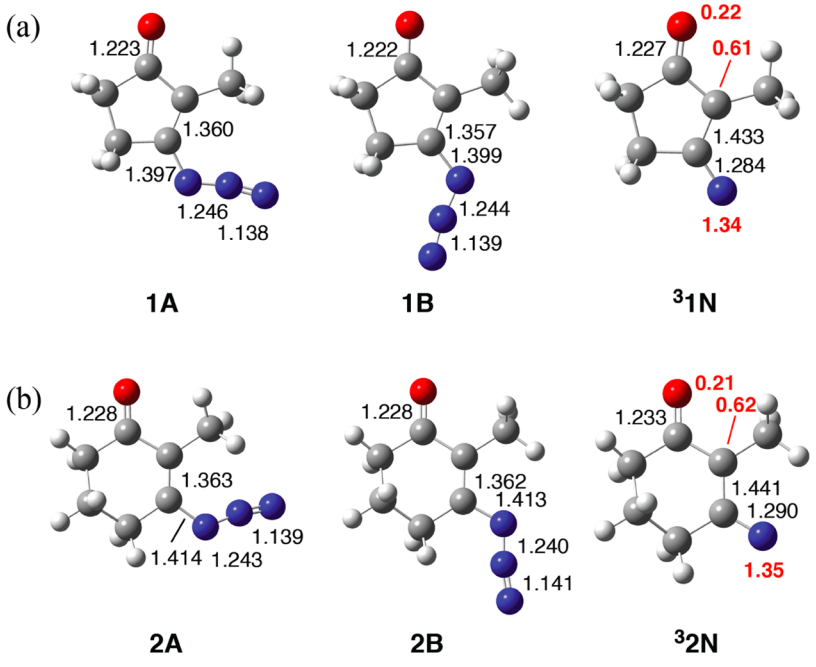

Figure 5. B3LYP/6-31+G(d)-optimized structures of (a) vinyl azide **1A**, **1B** and vinylnitrene ^{3}**1N** and (b) vinyl azide **2A**, **2B** and vinylnitrene ^{3}**2N**. Selected bond lengths (black) are in angstroms. Numbers in red are the calculated spin densities.

DOI: 10.1021/acs.joc.9b01191
J. Org. Chem. 2019, 84, 9215−9225

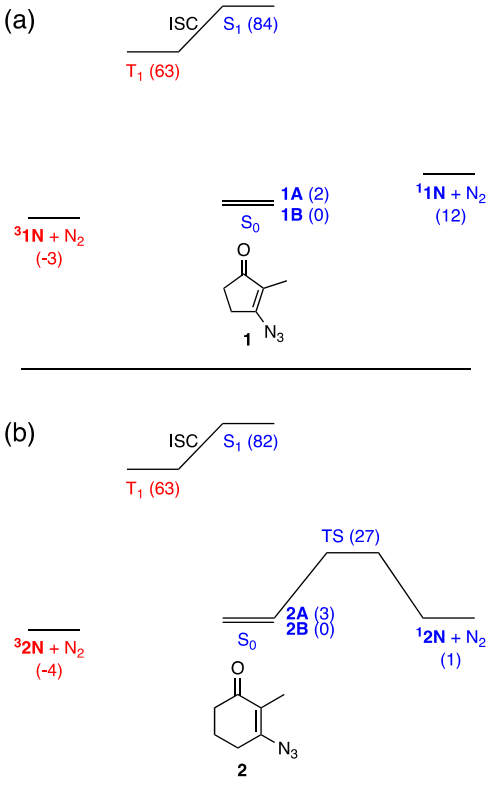

Figure 6. Calculated (B3LYP/6-31+G(d)) stationary points on the potential energy surface of vinyl azides (a) **1** and (b) **2**. Energies for S_1 and T_1 states are computed vertical excitation energies from the S_0 state of the azide. The calculated energies are expressed in kcal/mol. Singlet species are indicated in blue and triplet species in red.

vinylnitrene ^{3}**2N** is stable at cryogenic temperature, we theorize that intersystem crossing to ketenimine **6** and azirine **7** must be restricted. As in similar systems, we propose that intersystem crossing from vinylnitrene ^{3}**2N** requires rotation around the vinyl bond to achieve a conformation that makes intersystem crossing possible, but the ring structure restricts this rotation.

Spin density calculations (B3LYP/6-31+G(d)) showed that vinylnitrenes ^{3}**1N** and ^{3}**2N** have similar spin density patterns, with the N- and the α-C atoms exhibiting spin densities of ~1.3 and 0.6, respectively (Scheme 5). Further, the oxygen atom only has a small spin density of ~0.2. Thus, the unpaired electron density is mainly localized on the vinylnitrene chromophore, and the nitrenes have significant 1,3-biradical character.

The geometries of the open-shell singlet vinylnitrenes ^{1}**1N** and ^{1}**2N** were optimized using DFT with the broken symmetry method, as described in the literature.[34,35] The broken symmetry calculations, which were achieved using guess = mix as a keyword in Gaussian09, resulted in singlet vinylnitrenes ^{1}**1N** and ^{1}**2N** that are located 15 and 5 kcal/mol, respectively, above the corresponding triplet configurations. Furthermore, the total spin $\langle S^2 \rangle$ values of 1.005 and 1.014, respectively, suggested significant spin contamination from the triplet state.

Owing to the high spin contamination in the DFT calculations, the singlet and triplet vinylnitrenes were also computed using the CASSCF and CASPT2 methods (for more details, see the Experimental Section). At the CASPT2(6,6)/cc-pVDZ//CASSCF(6,6)/cc-pVDZ level, vinylnitrene ^{1}**1N** is predicted to lie 12.0 kcal/mol above ^{3}**1N**, and vinylnitrene ^{1}**2N** is computed to be 11.2 kcal/mol higher in energy than ^{3}**2N**. Thus, the computed singlet−triplet energy gaps of the vinylnitrenes are more consistent for the different ring sizes using CASPT2 than using B3LYP. One surprising finding was that ^{1}**2N** is not a potential minimum but rather a transition state (vide infra).

The calculated stationary points on the potential energy surface connections between vinylnitrenes ^{3}**1N** and ^{3}**2N** and the corresponding secondary photoproducts are displayed in Figure 7. The barriers for vinylnitrene ^{3}**1N** to cleave and form ketene **4** and ketone **5** are less than those connecting vinylnitrene ^{3}**2N** to ketene **9** and ketone **10**, which fits with vinylnitrene ^{3}**1N** being more photochemically reactive than vinylnitrene ^{3}**2N**. Diradicals **5BR** and **10BR** are ~22 kcal/mol more stable than their counterparts **4BR** and **9BR** because in **5BR** and **10BR**, the unpaired electron on N resides in an orbital that overlaps with the π-system of the enone moiety rather than in an in-plane p-orbital. In contrast, in **4BR** and **9BR**, an unpaired electron is localized in an in-plane p-orbital on N. For diradicals **4BR**, **5BR**, **9BR**, and **10BR**, the singlet and triplet states are nearly degenerate. In only one case were we unable to locate a local minimum, that of ^{1}**5BR**, because upon geometry optimization, the structure collapsed to a cyclic product (ketone **5**).

Figure 7 also shows relevant singlet species. Of particular note is our finding that ^{1}**2N** is not a minimum but rather a transition state for interconversion of two isomeric azirines, **7a** and **7b**. The nitrogen can bend to either face of the six-membered ring, giving rise to two azirines that differ in the conformation of the six-membered ring. This finding is consistent with the results of Banert et al., who were unable to locate a minimum for ^{1}**2N**.[36] Moreover, it is similar to the situation for the parent singlet vinylnitrene ($H_2C{=}CH{-}N$), which is a transition state for the formation of two mirror-image azirine products. The ca. 1 kcal/mol barrier for the transformation of vinylnitrene ^{1}**1N** to azirine **8** is consistent with the shallow nature of the potential surface in the vicinity of these singlet nitrenes, and the pattern that the nature of the stationary point can change depending on substituents or ring size.

DISCUSSION

From the experimental results, we conclude that intersystem crossing, S_1 to T_1, is more effective for vinyl azide **1** than for vinyl azide **2** based on the following considerations. Vinyl azide **2** forms significant amounts of azirine **7** and ketenimine **6** from its singlet excited state in competition with intersystem crossing to vinylnitrene ^{3}**2N**. In comparison, vinyl azide **1** forms only a small amount of ketenimine **3** concurrently with intersystem crossing to vinylnitrene ^{3}**1N**. Thus, the decreased ring size of vinyl azide **1** must enhance its intersystem crossing in comparison to that of vinyl azide **2**. Similar phenomena have been observed for aliphatic and aromatic ketone derivatives, as intersystem crossing is enhanced in strained cyclic compounds.[37,38]

The D/hc values for vinylnitrenes ^{3}**1N** and ^{3}**2N** are remarkably similar, indicating that these species are delocalized vinylnitrenes, as predicted by their calculated spin densities (Scheme 5). The E/hc values for vinylnitrenes ^{3}**1N** and ^{3}**2N** are less alike; presumably, the lower E/hc value for ^{3}**1N** is a reflection of it having less symmetry of the spin magnetic moments than ^{3}**2N**. A comparison of the zfs parameters of

DOI: 10.1021/acs.joc.9b01191
J. Org. Chem. 2019, 84, 9215−9225

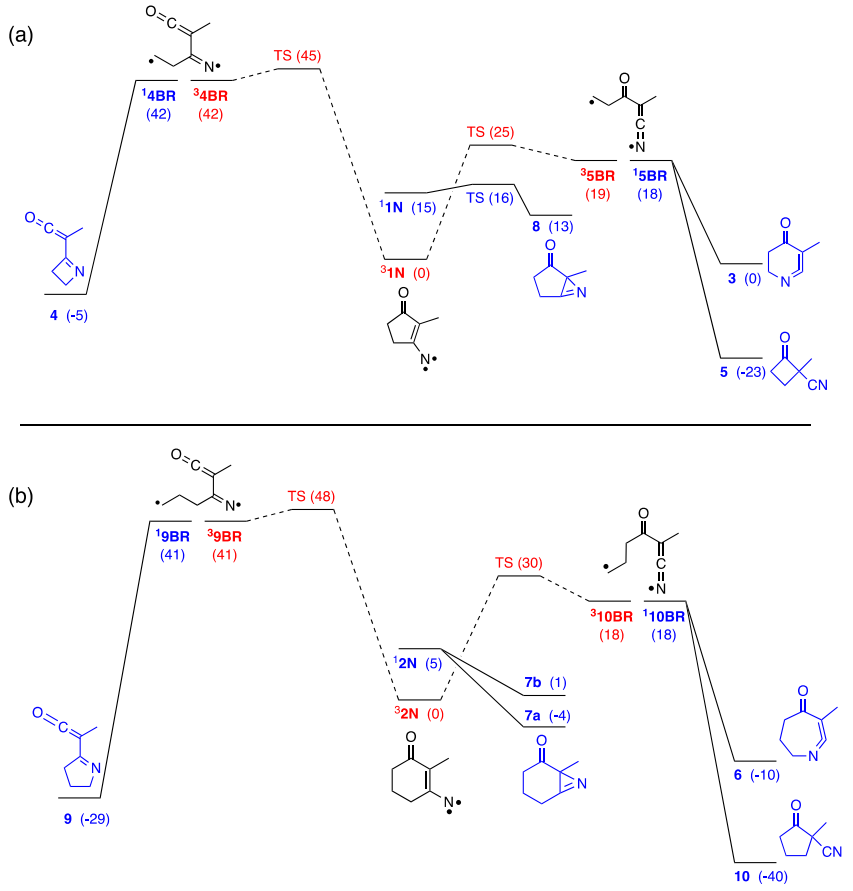

Figure 7. Calculated (B3LYP/6-31+G(d)) stationary points on the potential energy surface of vinylnitrenes (a) **1N** and (b) **2N**. The calculated energies are expressed in kcal/mol. Singlet species are indicated in blue and triplet species in red. Black structures are shown for species with both singlet and triplet states. No stationary point was located for ^{1}**5BR**, as it collapses to cyclic products upon optimization; thus, the energy indicated for ^{1}**5BR** is the singlet energy at the triplet geometry.

Scheme 5. zfs Values and Calculated Spin Densities (Shown in Red) of Cyclic Vinylnitrenes[a]

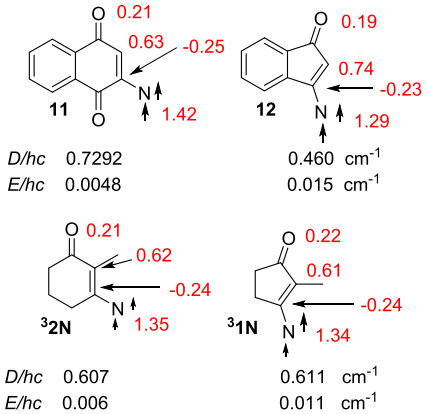

[a]Only spin densities greater than 0.15 are included; for more details, see the SI.

vinylnitrenes ^{3}**1N** and ^{3}**2N** to those of other cyclic vinylnitrenes such as ^{3}**11** and ^{3}**12** (Scheme 5) shows that vinylnitrenes ^{3}**1N** and ^{3}**2N** have more significant 1,3-biradical character than vinylnitrene ^{3}**11** but less than vinylnitrene ^{3}**12**. Even though the unpaired electrons of vinylnitrenes ^{3}**1N** and ^{3}**2N** are delocalized on the vinylnitrene chromophore with only a small contribution on the carbonyl oxygen, they have similar spin densities to vinylnitrene ^{3}**11**, highlighting that the unpaired electrons are not localized on the aromatic ring. In vinylnitrene ^{3}**12**, the spin density on the nitrogen atom is less prominent than for vinylnitrenes ^{3}**1N**, ^{3}**2N**, and ^{3}**11**; however, the spin density in vinylnitrene ^{3}**12** is not localized on the aromatic ring but delocalized on the α-carbon atom with a small contribution on the oxygen atom. The spin densities of triplet vinylnitrenes ^{3}**1N**, ^{3}**2N**, ^{3}**11**, and ^{3}**12** are delocalized on the vinylnitrene chromophore, and the aromatic rings have a little effect on the vinylnitrene character of ^{3}**11** and ^{3}**12**. Thus, both simple vinylnitrenes and vinylnitrenes with extended conjugated systems have similar unpaired electron densities.

Our results support those of Banert and co-workers,[36,39] who reported that direct photolysis of vinyl azide **1** at −50 °C yields products **13** and **14** (Scheme 6) and theorized that they were formed by the reaction of vinylnitrene ^{3}**1N** with other triplet vinylnitrene intermediates to form new C−N and N−N bonds. In contrast, they demonstrated that direct irradiation of vinyl azide **2** at −50 °C resulted in azirine **7**, whereas triplet sensitization with benzophenone resulted in products **15** and **16**, which are attributed to the dimerization of vinylnitrene ^{3}**2N**. Our studies support the notion that upon direct photolysis, vinyl azide **2** will mainly exhibit singlet reactivity in competition with intersystem crossing to vinylnitrene ^{3}**2N**, whereas vinyl azide **1** will react mainly on its triplet surface.

DOI: 10.1021/acs.joc.9b01191
J. Org. Chem. 2019, 84, 9215−9225

Scheme 6

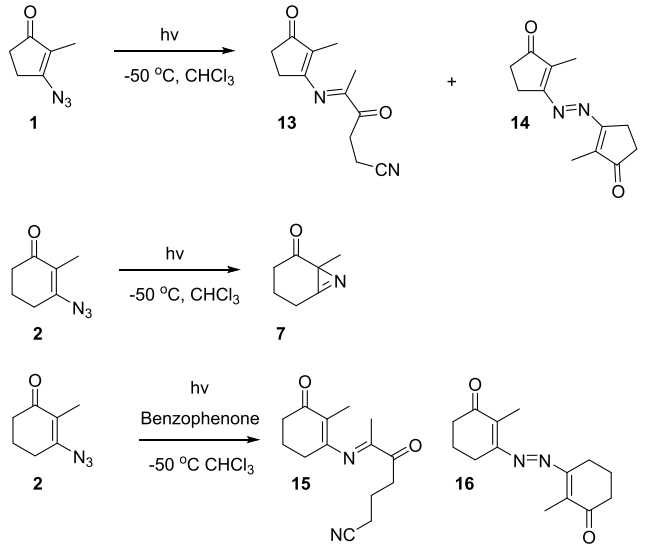

CONCLUSIONS

We have shown that direct irradiation of vinyl azides **1** and **2** at cryogenic temperature results in the formation of vinylnitrenes ^{3}**1N** and ^{3}**2N**, respectively, which are stable at cryogenic temperature. These triplet vinylnitrenes have significant 1,3-biradical character, as predicted by DFT calculations and verified with EPR spectroscopy. The strain of the five-membered ring in vinyl azide **1** enhances intersystem crossing to form T_1 of **1** and subsequently vinylnitrene ^{3}**1N**. In comparison, irradiation of vinyl azide **2** results in significant yields of singlet products in competition with intersystem crossing to form vinylnitrene ^{3}**2N**, which is photostable. Thus, the photoreactivities of vinyl azides **1** and **2** are different, because intersystem crossing is efficient in vinyl azide **1** but not in vinyl azide **2**. Thus, to successfully apply simple cyclic vinyl azides in synthetic applications, it is necessary to establish whether they react on their singlet or triplet surface.

EXPERIMENTAL SECTION

EPR Spectroscopy. Dilute solutions of vinyl azides **1** and **2** in anhydrous mTHF were prepared (100 and 80 mM, respectively) and then degassed via the freeze–pump–thaw method three times before recording EPR spectra using a Bruker X-band EPR E500 spectrometer. All measurements were performed at 10 K, unless otherwise stated. Temperature-dependence measurements were also collected after 10 min irradiation. The cyclic vinyl azides were irradiated using a mercury arc lamp (>250 nm).

UV–Vis Absorption Spectroscopy. Dilute solutions of vinyl azides **1** and **2** were prepared in anhydrous mTHF. All measurements were performed at 77 K. Vinyl azide **1** was irradiated with a xenon arc lamp with a borosilicate/Pyrex glass filter (>300 nm). Vinyl azide **2** was irradiated with an LED (~310 nm).

Matrix IR Spectroscopy. Matrix isolation of vinyl azide **1** was performed on a conventional equipment.[40] Argon was deposited at 22 K on a CsI window, and then argon and the sample were deposited at room temperature for 46 min under vacuum. The system was then cooled to 12 K before starting the measurement. The sample was irradiated through the quartz window with an LED (~310 nm). IR spectra were collected periodically at various irradiation times. Vinyl azide **2** was sublimed at 50 °C and deposited with argon at 22 K in the vacuum of a diffusion pump. The cryostat cold head was cooled to 8 K before irradiation. The matrix was irradiated with a xenon arc lamp through a 310–350 nm glass filter, and IR spectra were collected at various times. IR spectra were recorded from 450 to 4000 cm^{-1}, averaging 48 scans at 1 cm^{-1} resolution, using a PerkinElmer Spectrum One Fourier transform infrared (FT-IR) spectrometer. Spectra were recorded during and after matrix deposition.

Quantum Chemical Calculations. Geometries of all species were initially optimized at the B3LYP level of theory with the 6-31+G(d) basis set using the Gaussian09 program.[41−43] Calculated UV–vis spectra were obtained using TDDFT calculations with the incorporation of solvation using the IPCM model.[44−46] The calculated transition states were confirmed to contain one imaginary vibrational frequency by analytical determination of the second derivative of the energy with respect to the internal coordinates. Intrinsic reaction coordinate calculations were used to verify that the transition states were correlated with the proper reactants and products.[47,48] All DFT calculations were performed at the Ohio Supercomputer Center.

To obtain more accurate singlet–triplet energy gaps, the energies of the vinylnitrenes were computed at the CASPT2(6,6)/cc-pVDZ level,[49,50] using CASSCF(6,6)/cc-pVDZ-optimized geometries. The active space for these calculations consisted of the five π/π^* MOs plus the in-plane nonbonding MO (NBMO) on nitrogen. The electronic transitions of the triplet vinylnitrenes were computed using a combination of state-averaged CASSCF and multistate CASPT2 calculations on the B3LYP/6-31+G(d) structures. The 12-electron, 11-orbital active space in these CASPT2(12,11)/cc-pVDZ calculations consisted of all of the π/π^* MOs, the in-plane NBMO on nitrogen, plus three σ/σ^* pairs (combinations of the C–O σ bond, the Cα–Cβ σ bond, and the σ bond between the carbonyl carbon and the α carbon). Using a slightly smaller active space of 10 electrons and 10 orbitals did not significantly affect the results. The excited-state CASPT2 calculations employed level shift parameter of 0.2 to eliminate intruder states. The CASSCF and CASPT2 calculations were performed with Molcas 8.2.[51] The MOs were visualized with Molden.[52]

Preparation of Vinyl Azides 1 and 2.[53] *Synthesis of 3-Chloro-2-methylcyclopent-2-en-1-one (Step 1).* In a round-bottom flask, 2-methylcyclopentane-1,3-dione (1.0 g, 8.9 mmol) was dissolved in 25 mL of chloroform. While stirring, trichlorophosphane (PCl_3; 1.3 mL, 15 mmol) was added dropwise, and then the mixture was refluxed for approximately 6 h and allowed to stir with no heat for an additional 13 h. The reaction mixture was placed in an ice bath to cool, then poured into 30 mL of cold deionized water and extracted with cold diethyl ether (2 × 50 mL). The extracted layers were washed with 20% aqueous NaOH and brine, and then dried over $MgSO_4$. The filtrate was dried under an air stream to give an oil of 3-chloro-2-methylcyclopent-2-en-1-one (0.896 g, 6.76 mmol, 75% yield). The oil was used for the next reaction step without any further purification. Chloro-2-methylcyclopent-2-en-1-one was characterized by ^{1}H NMR and FT-IR spectroscopy, and the obtained spectra agreed with those published in the literature.[53] ^{1}H NMR (400 MHz, $CDCl_3$) δ 2.79–2.71 (m, 3H), 2.56–2.51 (m, 2H), 1.65 (t, J = 1.9 Hz, 3H) ppm. IR (neat): 1706, 1641 cm^{-1}.

Synthesis of 3-Azido-2-methylcyclopent-2-en-1-one (Step 2). 3-Chloro-2-methylcyclopent-2-en-1-one (0.65 g, 4.9 mmol) was dissolved in 6 mL of methanol and 2 mL of deionized water while stirring in a 250 mL round-bottom flask. NaN_3 (0.49 g, 7.5 mmol) was added, and the mixture was stirred for ~41.5 h. The reaction mixture was extracted with diethyl ether (3 × 25 mL), washed with deionized water, and then dried over $MgSO_4$. The filtrate was dried under high vacuum to obtain a brown oil of 3-azido-2-methylcyclopent-2-en-1-one (**1**; 0.30 g, 2.2 mmol, 44% yield). The oil was used for cryogenic experiments without purification. Vinyl azide **1** was characterized by ^{1}H NMR and IR spectroscopy, and the observed spectra agreed with those published in the literature.[53] ^{1}H NMR (400 MHz, $CDCl_3$) δ 2.79–2.70 (m, 2H), 2.58–2.49 (m, 2H), 1.65 (q, J = 1.6 Hz, 3H) ppm. IR (neat): 2012, 1690, 1629 cm^{-1}.

Synthesis of 3-Chloro-2-methylcyclohex-2-en-1-one (Step 1). In a round-bottom flask, 2-methylcyclohexane-1,3-dione (5.0 g, 40 mmol) was dissolved in 50 mL of chloroform. While stirring, PCl_3 (10 mL, 114 mmol) was added dropwise, and the mixture was refluxed for approximately 4 h. The reaction mixture was placed in an ice bath to

DOI: 10.1021/acs.joc.9b01191
J. Org. Chem. 2019, 84, 9215–9225

cool and then poured into 30 mL of cold deionized water and extracted with cold diethyl ether (25 mL). The extracted layers were washed with 10% aqueous NaOH and brine, dried over $MgSO_4$, and then the filtrate was concentrated in a rotary vacuum evaporator to give an oil of 3-chloro-2-methylcyclohex-2-en-1-one (2.5 g, 18 mmol, 44% yield). The oil was used for the next reaction step without further purification. 3-Chloro-2-methylcyclohex-2-en-1-one was characterized by ^{1}H NMR and FT-IR spectroscopy, and the obtained spectra agreed with those published in the literature.[53] ^{1}H NMR (400 MHz, $CDCl_3$): δ 2.75 (tq, J = 6.1, 2.0 Hz, 2H), 2.50−2.41 (m, 2H), 2.04 (dq, J = 8.0, 6.4 Hz, 2H), 1.91 (t, J = 2.0 Hz, 3H) ppm. IR (neat): 1674, 1626, 1431, 986 cm^{-1}.

Synthesis of 3-Azido-2-methylcyclohex-2-en-1-one (Step 2). 3-Chloro-2-methylcyclohex-2-en-1-one (1.8 g, 12 mmol) was dissolved in 10 mL of methanol and 5 mL of deionized water by stirring. NaN_3 (1.3 g, 20 mmol) was added, and the mixture was stirred for ∼4 days (95 h). The reaction mixture was extracted with diethyl ether (25 mL), washed with deionized water, and dried over $MgSO_4$. The solvent was removed under vacuum to yield an oil of 3-azido-2-methylcyclohex-2-en-1-one (**2**; 1.7 g, 11 mmol, 94% yield). This oil was used for cryogenic experiments without any further purification. Vinyl azide **2** was characterized by ^{1}H NMR and FT-IR spectroscopy, and the obtained spectra agreed with those published in the literature.[53] ^{1}H NMR (400 MHz, $CDCl_3$): δ 2.62 (tq, J = 6.0, 1.8 Hz, 2H), 2.41 (dd, J = 7.4, 6.0 Hz, 2H), 2.08 (d, J = 6.4 Hz, 2H), 1.73 (t, J = 1.8 Hz, 3H) ppm. IR (neat): 2092, 1652, 1615 cm^{-1}.

■ ASSOCIATED CONTENT

Supporting Information

The Supporting Information is available free of charge on the ACS Publications website at DOI: 10.1021/acs.joc.9b01191.

IR and ^{1}H NMR spectra of vinyl azides **1**, **2** and their chloro-precursors; optimized structures of **1**, ^{1}**1N**, ^{3}**1N**, **2**, ^{1}**2N**, ^{3}**2N**, and **3**−**9**; CASSCF and CASPT2 absolute energies of nitrenes ^{1}**1N**, ^{3}**1N**, ^{1}**2N**, and ^{3}**2N** (PDF)

■ AUTHOR INFORMATION

Corresponding Author

*E-mail: anna.gudmundsdottir@uc.edu.

ORCID

William L. Karney: 0000-0003-0976-742X
Manabu Abe: 0000-0002-2013-4394
Bruce S. Ault: 0000-0003-3355-1960
Anna D. Gudmundsdottir: 0000-0002-5420-4098

Notes

The authors declare no competing financial interest.

■ ACKNOWLEDGMENTS

This work was generously supported by the NSF (CHE-1464694, CHE-1565793, and CHE-1800140) and the Ohio Supercomputer Center. D.M.G. is grateful for the Ann P. Villalobos Fellowship. M.A. gratefully acknowledges financial support by JSPS KAKENHI (Grant No. JP17H03022).

■ REFERENCES

(1) Bräse, S.; Gil, C.; Knepper, K.; Zimmermann, V. Organic Azides: An Exploding Diversity of a Unique Class of Compounds. *Angew. Chem., Int. Ed.* **2005**, *44*, 5188−5240.

(2) Fu, J.; Zanoni, G.; Anderson, E. A.; Bi, X. α-Substituted Vinyl Azides: An Emerging Functionalized Alkene. *Chem. Soc. Rev.* **2017**, *46*, 7208−7228.

(3) Xie, S.; Lopez, S. A.; Ramström, O.; Yan, M.; Houk, K. N. 1,3-Dipolar Cycloaddition Reactivities of Perfluorinated Aryl Azides with Enamines and Strained Dipolarophiles. *J. Am. Chem. Soc.* **2015**, *137*, 2958−2966.

(4) Agnew, H. D.; Rohde, R. D.; Millward, S. W.; Nag, A.; Yeo, W.-S.; Hein, J. E.; Pitram, S. M.; Tariq, A. A.; Burns, V. M.; Krom, R. J.; Fokin, V. V.; Sharpless, K. B.; Heath, J. R. Iterative In Situ Click Chemistry Creates Antibody-Like Protein-Capture Agents. *Angew. Chem., Int. Ed.* **2009**, *48*, 4944−4948.

(5) Tornøe, C. W.; Christensen, C.; Meldal, M. Peptidotriazoles on Solid Phase: [1,2,3]-Triazoles by Regiospecific Copper(I)-Catalyzed 1,3-Dipolar Cycloadditions of Terminal Alkynes to Azides. *J. Org. Chem.* **2002**, *67*, 3057−3064.

(6) Rostovtsev, V. V.; Green, L. G.; Fokin, V. V.; Sharpless, K. B. A Stepwise Huisgen Cycloaddition Process: Copper(I)-Catalyzed Regioselective "Ligation" of Azides and Terminal Alkynes. *Angew. Chem., Int. Ed.* **2002**, *41*, 2596−2599.

(7) Kolb, H. C.; Finn, M. G.; Sharpless, K. B. Click Chemistry: Diverse Chemical Function from a Few Good Reactions. *Angew. Chem., Int. Ed* **2001**, *40*, 2004−2021.

(8) Huisgen, R. 1,3-Dipolar Cycloadditions. Past and Future. *Angew. Chem., Int. Ed* **1963**, *2*, 565−598.

(9) Khlebnikov, A. F.; Novikov, M. S. Recent Advances in 2*H*-Azirine Chemistry. *Tetrahedron* **2013**, *69*, 3363−3401.

(10) Zhou, H.; Shen, M.-H.; Xu, H.-D. Evolution of the Aza-Diels−Alder Reaction of 2*H*-Azirines. *Synlett* **2016**, *27*, 2171−2177.

(11) Oelgemöller, M. Solar Photochemical Synthesis: From the Beginnings of Organic Photochemistry to the Solar Manufacturing of Commodity Chemicals. *Chem. Rev.* **2016**, *116*, 9664−9682.

(12) Zhao, F.; Cambié, D.; Hessel, V.; Debije, M. G.; Noël, T. Real-Time Reaction Control for Solar Production of Chemicals under Fluctuating Irradiance. *Green Chem.* **2018**, *20*, 2459−2464.

(13) Huang, X.; Webster, R. D.; Harms, K.; Meggers, E. Asymmetric Catalysis with Organic Azides and Diazo Compounds Initiated by Photoinduced Electron Transfer. *J. Am. Chem. Soc.* **2016**, *138*, 12636−12642.

(14) Farney, E. P.; Yoon, T. P. Visible-Light Sensitization of Vinyl Azides by Transition-Metal Photocatalysis. *Angew. Chem., Int. Ed.* **2014**, *53*, 793−797.

(15) Scriven, E. F. V.; Turnbull, K. Azides: Their Preparation and Synthetic Uses. *Chem. Rev.* **1988**, *88*, 297−368.

(16) Scriven, E. F. V., Ed.; *Azides and Nitrenes: Reactivity and Utility*; Academic Press, Inc.: Orlando, FL, 1984.

(17) Platz, M. S. Nitrenes. In *Reactive Intermediate Chemistry*; Moss, R. A., Platz, M. S., Jones, M., Jr., Eds.; John Wiley & Sons, Inc.: Hoboken, NJ, 2004; pp 501−559.

(18) Bucher, G. Photochemical Reactivity of Azides. In *CRC Handbook of Organic Photochemistry and Photobiology*, 2nd ed.; Horspool, W. M., Lenci, F., Eds.; CRC Press: Boca Raton, FL, 2004; pp 44/1−44/31.

(19) Osisioma, O.; Chakraborty, M.; Ault, B. S.; Gudmundsdottir, A. D. Wavelength-Dependent Photochemistry of 2-Azidovinylbenzene and 2-Phenyl-2*H*-azirine. *J. Mol. Struct.* **2018**, *1172*, 94−101.

(20) Rajam, S.; Jadhav, A. V.; Li, Q.; Sarkar, S. K.; Singh, P. N. D.; Rohr, A.; Pace, T. C. S.; Li, R.; Krause, J. A.; Bohne, C.; Ault, B. S.; Gudmundsdottir, A. D. Triplet Sensitized Photolysis of a Vinyl Azide: Direct Detection of a Triplet Vinyl Azide and Nitrene. *J. Org. Chem.* **2014**, *79*, 9325−9334.

(21) Weragoda, G. K.; Das, A.; Sarkar, S. K.; Sriyarathne, H. D. M.; Zhang, X.; Ault, B. S.; Gudmundsdottir, A. D. Singlet Photoreactivity of 3-Methyl-2-phenyl-2*H*-azirine. *Aust. J. Chem.* **2017**, *70*, 413−420.

(22) Gamage, D. W.; Li, Q.; Ranaweera, R. A. A. U.; Sarkar, S. K.; Weragoda, G. K.; Carr, P. L.; Gudmundsdottir, A. D. Vinylnitrene Formation from 3,5-Diphenyl-isoxazole and 3-Benzoyl-2-phenyl-azirine. *J. Org. Chem.* **2013**, *78*, 11349−11356.

(23) Rajam, S.; Murthy, R. S.; Jadhav, A. V.; Li, Q.; Keller, C.; Carra, C.; Pace, T. C. S.; Bohne, C.; Ault, B. S.; Gudmundsdottir, A. D. Photolysis of (3-Methyl-2*H*-azirin-2-yl)-phenylmethanone: Direct Detection of a Triplet Vinylnitrene Intermediate. *J. Org. Chem.* **2011**, *76*, 9934−9945.

(24) Zhang, X.; Sarkar, S. K.; Weragoda, G. K.; Rajam, S.; Ault, B. S.; Gudmundsdottir, A. D. Comparison of the Photochemistry of 3-

DOI: 10.1021/acs.joc.9b01191
J. Org. Chem. 2019, 84, 9215−9225

Methyl-2-phenyl-2*H*-azirine and 2-Methyl-3-phenyl-2*H*-azirine. *J. Org. Chem.* **2014**, *79*, 653−663.
(25) Sarkar, S. K.; Sawai, A.; Kanahara, K.; Wentrup, C.; Abe, M.; Gudmundsdottir, A. D. Direct Detection of a Triplet Vinylnitrene, 1,4-Naphthoquinone-2-ylnitrene, in Solution and Cryogenic Matrices. *J. Am. Chem. Soc.* **2015**, *137*, 4207−4214.
(26) Sarkar, S. K.; Osisioma, O.; Karney, W. L.; Abe, M.; Gudmundsdottir, A. D. Using Molecular Architecture to Control the Reactivity of a Triplet Vinylnitrene. *J. Am. Chem. Soc.* **2016**, *138*, 14905−14914.
(27) Wasserman, E.; Snyder, L. C.; Yager, W. A. ESR of the Triplet States of Randomly Oriented Molecules. *J. Chem. Phys.* **1964**, *41*, 1763−1772.
(28) Kvaskoff, D.; Bednarek, P.; George, L.; Waich, K.; Wentrup, C. Nitrenes, Diradicals, and Ylides. Ring Expansion and Ring Opening in 2-Quinazolylnitrenes. *J. Org. Chem.* **2006**, *71*, 4049−4058.
(29) Wentrup, C.; Kvaskoff, D. 1,5-(1,7)-Biradicals and Nitrenes Formed by Ring Opening of Hetarylnitrenes. *Aust. J. Chem.* **2013**, *66*, 286−296.
(30) Wentrup, C. Flash Vacuum Pyrolysis of Azides, Triazoles, and Tetrazoles. *Chem. Rev.* **2017**, *117*, 4562−4623.
(31) Foresman, J. B.; Frisch, Æ. *Exploring Chemistry with Electronic Structure Methods*, 2nd ed.; Gaussian Inc.: Pittsburgh, PA, 1996.
(32) Kniep, C. S.; Padias, A. B.; Hall, H. K., Jr. Cycloaddition Reactions of Ketene Diethyl Acetal toward the Synthesis of Cyclobutene Monomers. *Tetrahedron* **2000**, *56*, 4279−4288.
(33) Chapman, O. L.; Le Roux, J. P. 1-Aza-1,2,4,6-cycloheptatetraene. *J. Am. Chem. Soc.* **1978**, *100*, 282−285.
(34) Noodleman, L.; Baerends, E. J. Electronic Structure, Magnetic Properties, ESR, and Optical Spectra for 2-Fe Ferredoxin Models by LCAO−Xα Valence Bond Theory. *J. Am. Chem. Soc.* **1984**, *106*, 2316−2327.
(35) Yamaguchi, K.; Jensen, F.; Dorigo, A.; Houk, K. N. A Spin Correction Procedure for Unrestricted Hartree-Fock and Møller-Plesset Wavefunctions for Singlet Diradicals and Polyradicals. *Chem. Phys. Lett.* **1988**, *149*, 537−542.
(36) Banert, K.; Meier, B.; Penk, E.; Saha, B.; Würthwein, E.-U.; Grimme, S.; Rüffer, T.; Schaarschmidt, D.; Lang, H. Highly Strained 2,3-Bridged 2*H*-Azirines at the Borderline of Closed-Shell Molecules. *Chem. − Eur. J.* **2011**, *17*, 1128−1136.
(37) Yang, N.-C.; Feit, E. D.; Hui, M. H.; Turro, N. J.; Dalton, J. C. Photochemistry of Di-*tert*-butyl Ketone and Structural Effects on the Rate and Efficiency of Intersystem Crossing of Aliphatic Ketones. *J. Am. Chem. Soc.* **1970**, *92*, 6974−6976.
(38) McGarry, P. F.; Doubleday, C. E., Jr.; Wu, C.-H.; Staab, H. A.; Turro, N. J. UV−Vis Absorption Studies of Singlet to Triplet Intersystem Crossing Rates of Aromatic Ketones: Effects of Molecular Geometry. *J. Photochem. Photobiol., A* **1994**, *77*, 109−117.
(39) Banert, K.; Meier, B. Synthesis and Reactions of Highly Strained 2,3-Bridged 2*H*-Azirines. *Angew. Chem., Int. Ed.* **2006**, *45*, 4015−4019.
(40) Ault, B. S. Infrared Spectra of Argon Matrix-Isolated Alkali Halide Salt/Water Complexes. *J. Am. Chem. Soc.* **1978**, *100*, 2426−2433.
(41) Becke, A. D. Density-Functional Thermochemistry. III. The Role of Exact Exchange. *J. Chem. Phys.* **1993**, *98*, 5648−5652.
(42) Lee, C.; Yang, W.; Parr, R. G. Development of the Colle-Salvetti Correlation-Energy Formula into a Functional of the Electron Density. *Phys. Rev. B* **1988**, *37*, 785−789.
(43) Frisch, M. J.; Trucks, G. W.; Schlegel, H. B.; Scuseria, G. E.; Robb, M. A.; Cheeseman, J. R.; Scalmani, G.; Barone, V.; Mennucci, B.; Petersson, G. A.; Nakatsuji, H.; Caricato, M.; Li, X.; Hratchian, H. P.; Izmaylov, A. F.; Bloino, J.; Zheng, G.; Sonnenberg, J. L.; Hada, M.; Ehara, M.; Toyota, K.; Fukuda, R.; Hasegawa, J.; Ishida, M.; Nakajima, T.; Honda, Y.; Kitao, O.; Nakai, H.; Vreven, T.; Montgomery, J. A., Jr.; Peralta, J. E.; Ogliaro, F.; Bearpark, M.; Heyd, J. J.; Brothers, E.; Kudin, K. N.; Staroverov, V. N.; Kobayashi, R.; Normand, J.; Raghavachari, K.; Rendell, A.; Burant, J. C.; Iyengar, S. S.; Tomasi, J.; Cossi, M.; Rega, N.; Millam, J. M.; Klene, M.; Knox, J. E.; Cross, J. B.; Bakken, V.; Adamo, C.; Jaramillo, J.; Gomperts, R.; Stratmann, R. E.; Yazyev, O.; Austin, A. J.; Cammi, R.; Pomelli, C.; Ochterski, J. W.; Martin, R. L.; Morokuma, K.; Zakrzewski, V. G.; Voth, G. A.; Salvador, P.; Dannenberg, J. J.; Dapprich, S.; Daniels, A. D.; Farkas, Ö.; Foresman, J. B.; Ortiz, J. V.; Cioslowski, J.; Fox, D. J. *Gaussian 09*; Gaussian, Inc.: Wallingford, CT, 2009.
(44) Bauernschmitt, R.; Ahlrichs, R. Treatment of Electronic Excitations within the Adiabatic Approximation of Time Dependent Density Functional Theory. *Chem. Phys. Lett.* **1996**, *256*, 454−464.
(45) Foresman, J. B.; Head-Gordon, M.; Pople, J. A.; Frisch, M. J. Toward a Systematic Molecular Orbital Theory for Excited States. *J. Phys. Chem. A* **1992**, *96*, 135−149.
(46) Stratmann, R. E.; Scuseria, G. E.; Frisch, M. J. An Efficient Implementation of Time-Dependent Density-Functional Theory for the Calculation of Excitation Energies of Large Molecules. *J. Chem. Phys.* **1998**, *109*, 8218−8224.
(47) Gonzalez, C.; Schlegel, H. B. An Improved Algorithm for Reaction Path Following. *J. Chem. Phys.* **1989**, *90*, 2154−2161.
(48) Gonzalez, C.; Schlegel, H. B. Reaction Path Following in Mass-Weighted Internal Coordinates. *J. Phys. Chem. A* **1990**, *94*, 5523−5527.
(49) Andersson, K.; Malmqvist, P.-Å.; Roos, B. O. Second-Order Perturbation Theory with a Complete Active Space Self-Consistent Field Reference Function. *J. Chem. Phys.* **1992**, *96*, 1218−1226.
(50) Dunning, T. H., Jr. Gaussian Basis Sets for Use in Correlated Molecular Calculations. I. The Atoms Boron through Neon and Hydrogen. *J. Chem. Phys.* **1989**, *90*, 1007−1023.
(51) Aquilante, F.; Autschbach, J.; Carlson, R. K.; Chibotaru, L. F.; Delcey, M. G.; De Vico, L.; Galván, I. F.; Ferré, N.; Frutos, L. M.; Gagliardi, L.; Garavelli, M.; Giussani, A.; Hoyer, C. E.; Li Manni, G.; Lischka, H.; Ma, D.; Malmqvist, P. Å.; Müller, T.; Nenov, A.; Olivucci, M.; Pedersen, T. B.; Peng, D.; Plasser, F.; Pritchard, B.; Reiher, M.; Rivalta, I.; Schapiro, I.; Segarra-Martí, J.; Stenrup, M.; Truhlar, D. G.; Ungur, L.; Valentini, A.; Vancoillie, S.; Veryazov, V.; Vysotskiy, V. P.; Weingart, O.; Zapata, F.; Lindh, R. MOLCAS 8: New Capabilities for Multiconfigurational Quantum Chemical Calculations across the Periodic Table. *J. Comput. Chem.* **2016**, *37*, 506−541.
(52) Schaftenaar, G.; Noordik, J. H. Molden: A Pre- and Post-Processing Program for Molecular and Electronic Structures. *J. Comput.-Aided Mol. Des.* **2000**, *14*, 123−134.
(53) Tamura, Y.; Kato, S.; Yoshimura, Y.; Nishimura, T.; Kita, Y. Rearrangement in Dihydroresorcinol Derivatives. XI. Photolysis and Thermolysis of 3-Azido-2-cyclohexen-1-ones and 2-Cyclopenten-1-ones. *Chem. Pharm. Bull.* **1974**, *22*, 1291−1296.

DOI: 10.1021/acs.joc.9b01191
J. Org. Chem. 2019, 84, 9215−9225